Available online at www.sciencedirect.com
ScienceDirect
Journal of the European Ceramic Society 27 (2007) 3287–3292
www.elsevier.com/locate/jeurceramsoc

# Polysilazane-derived antibacterial silver–ceramic nanocomposites

Vadym Bakumov [a,b], Katja Gueinzius [c], Corinna Hermann [c], Marcus Schwarz [a], Edwin Kroke [a,*]

[a] *Institute of Inorganic Chemistry, TU Bergakademie Freiberg, Leipziger Strasse 29, 09596 Freiberg, Germany*
[b] *Department of Chemistry, University of Konstanz, Universitätstrasse 10, 78467 Konstanz, Germany*
[c] *Department of Biochemical Pharmacology, University of Konstanz, Universitätstrasse 10, 78467 Konstanz, Germany*

Received 1 September 2006; received in revised form 22 December 2006; accepted 7 January 2007
Available online 26 February 2007

**Abstract**

Functional ceramic composites consisting of a dispersion of silver nanoparticles in a silicon (carbon)nitride matrix (*nc*-Ag/Si(C)N) were prepared via the polymer–ceramic route. Mixtures of 3 wt% as-synthesized Ag nanoparticles with a commercial polysilazane were pyrolysed under flowing nitrogen and/or ammonia. Bulk samples as well as coatings were investigated. Powder X-ray diffraction (XRD), transmission electron microscopy (TEM), thermal analysis (TGA, DTA), absorption spectroscopy (UV–vis) and infra red (IR) spectroscopy were used to characterize the products. The results indicate that the silver nanoparticles do not influence the cross-linking and pyroylsis process of the polysilazane precursor. At temperatures in the range of 800–1000 °C (H)Si(C)N matrices are obtained, which contain silver particles with an average size of 5–7 nm. Antibacterial tests on the pyrolysed material revealed strong activity against *Escherichia coli* and *Staphylococcus aureus*, suggesting the composites to be promising candidates for applications in fields such as the biomedical or food industries.


*Keywords:* Films; Nanocomposites; Nitrides; Carbides; Biomedical applications

## 1. Introduction

Antibacterial ceramics have attracted significant attention in recent years.[1–4] These ceramics have been predominantly prepared via sol–gel routes,[1–4] using silver as the antibacterial component.[1,2,4] However, iron and zinc have also been used as antibacterial ferrite ceramic materials for suppressing bacterial growth in water tanks.[5] Pure anatase ($TiO_2$) ceramics were also examined.[3] Among these active ingredients, silver is most promising for applications such as bone replacement and wastewater treatment due to its non-toxicity and biocompatibility.

In order to explore and utilize various effects induced by scaling the size of materials to the nano-level, plenty of wet-chemical methods to produce metal nanoparticles have been developed.[6–9] From the ancient red glass, via the classical photography techniques until now, the production, investigation and use of noble metal colloids plays a prominent role in materials science and technology.[10] One of the reasons for the revived interest is related to the optical properties of noble metal nanoparticles as a result of quantum confinement phenomena.[11]

Polymer-derived ceramics are under continued intensive research by many groups.[12] Pyrolysis of inorganic polymers at relatively low temperatures offers an attractive route to non-oxide ceramics with pre-defined composition and near-net shape. Compared to the classical sintering, this route is either an alternative, a complement or even the only possibility when it comes to ceramic coatings and fibres. Depending on the elemental composition of the inorganic polymer used as a starting material and controlled by the pyrolysis parameters, in particular temperature and atmosphere, various element combinations from pure stoichiometric binary (crystalline) phases to complicated multinary compositions are accessible. Frequently used precursor systems are silicon-based polymers such as polysilanes $(RR'Si)_n$ and/or polycarbosilanes for silicon carbide ceramics,[13] polysiloxanes $(RR'SiO)_n$ and/or polysilsesquioxanes $(RSiO_{1.5})_n$ for Si/C/O ceramics,[14] as well as polysilazanes $(RR'SiNR'')_n$ for Si/C, Si/N and Si/C/N materials,[15] to name just

* Corresponding author. Tel.: +49 3731 39 3174; fax: +49 3731 39 4058.
*E-mail address:* kroke@chemie.tu-freiberg.de (E. Kroke).

0955-2219/$ – see front matter © 2007 Elsevier Ltd. All rights reserved.
doi:10.1016/j.jeurceramsoc.2007.01.004

a few examples. In the present study, we used the versatility of this precursor technique to synthesize *nc*-Ag/Si(C)N composite ceramics from a commercially available polysilazane and examined its antibacterial properties.

## 2. Experimental

### 2.1. Chemicals and materials

A commercially available liquid polysilazane, Ceraset® VL20 (KION Corp. Pennsylvania, USA),[16] silver acetate (99% purity, ABCR), oleylamine and 1,1′-azobis-(cyclohexancarbonitrile) (Sigma–Aldrich) were used as purchased without further purification. Analytical grade toluene (Acros) and acetone (VWR) were used.

### 2.2. Synthesis techniques

Silver nanoparticles were synthesized similar to previously described methods.[6,7] In a typical procedure, 313 mg of silver acetate were dissolved in a solution of 10 ml of oleylamine and 10 ml of toluene, heated to 111 °C, refluxed for several hours and left to cool down to room temperature. Subsequently, 50 ml of acetone were added and the flocculated particles were separated by centrifugation at 2000 rpm. Finally the silver nanoparticles were redispersed in toluene and an aliquot corresponding to 30 mg of silver was added dropwise and under stirring to a boiling solution of 1 g polysilazane in 2 ml of toluene. The mixture was left to cool to ambient temperature and used for dip-coating and spin-coating procedures on quartz and steel substrates. For the characterization of bulk-composites, the solvent was removed *in vacuo*, then 10 mg of 1,1′-azo-1-bis(cyclohexanecarbonitrile) was added under stirring and the mixture was heated to 150 °C for cross-linking. Thin film samples were cross-linked at 290 °C and pyrolysed at 700, 800, 900 and 1000 °C in a quartz tube under flowing ammonia and/or nitrogen using a heating rate of 100 °C/h. The bulk samples were pyrolysed analogously. The maximal temperature was maintained for 1 h.

### 2.3. Characterization

Absorption spectra (UV–vis) were obtained on a Varian Cary 50 Spectrometer. X-ray diffraction (XRD) data were collected on a Guiner-type diffractometer (Huber G670) with an image plate, using Cu $K\alpha_1$ radiation (0.154056 nm). Transmission electron microscopy (TEM) was performed on a Zeiss EM 900 with accelerating voltage of 80 kV. To follow the interaction between the polymer and the nanoparticles highly diluted solutions/suspensions in toluene were mixed and dropped on carbon-coated TEM grid. Ceramic bulk samples were crushed and ceramic coatings were scraped off from the substrate. The resulting powders were dispersed in methanol and dropped on the TEM grid. For the thermogravimetric analysis (TGA) coupled with differential thermal analysis (DTA) a Netzsch STA 429 was used at a heating rate of 5 K/min under flowing nitrogen.

### 2.4. Antibacterial tests

The *nc*-Ag/Si(C)N nanocomposite samples—rinsed with nitric acid and with distilled water and uncoated quartz plate reference samples were placed into sterile Petri dishes. Each of these samples was treated on the surface with 50 μl of a suspension containing $10^8$ bacteria/ml. The humidity in the Petri dishes was kept constant by a paper, wetted with 0.9% solution of NaCl. The samples were left at 37 °C for 4 h (*Staphylococcus aureus*) and for 16 h (*Escherichia coli*) and washed with 5 ml 0.9% NaCl solution in the sterile bottle. The obtained solution was diluted subsequently by factor 10 and 100 and a portion of 100 μl was distributed on the surface of agar plates. After 18 h of incubation at 37 °C, the number of grown colonies was determined.

## 3. Results and discussion

### 3.1. Silver nanoparticle synthesis and ceramic precursor selection

A major aim of the present work was to obtain a new type of composite material in which silver nanopaticles are distributed in an amorphous, covalent, polymer derived Si/C/N matrix. Due to positive earlier results with the liquid poly(ureamethylvinyl)silazane Ceraset®,[17] we chose the very similar poly(methylvinyl)silazane Ceraset® VL20 as the ceramic matrix precursor (Fig. 1). Upon pyrolysis at temperatures around 1000 °C under an argon atmosphere it produces an amorphous Si/C/N ceramic matrix. Pyrolysis under ammonia leads to silicon nitride ceramics.

However, first attempts to mix the liquid Ceraset® VL20 or its solutions in organic solvents with silver salts also dissolved in organic solvents failed. Uncontrollable strong exothermic reactions occurred. Thus, we concluded that the silver ions are spontaneously reduced upon mixing with the silazane to form precipitates of elemental silver. It is known that the reduction activity of Si–H units is amplified in the presence of amines creating hyper-coordinated silicon centers and very reactive silicon hydride groups.[18] In the case of the $Ag^+$/[–RR′Si-NH–] system which we used here, an *in situ* amplification due to interaction of the electron lone pair of the nitrogen atoms with vacant $\sigma^*$- or d-molecular orbitals located on the silicon atoms may be responsible for the observed reaction.

Therefore, we chose another approach based on presynthesized silver nanoparticles, which were introduced into the precursor polymer. The synthesis of the Ag particles was

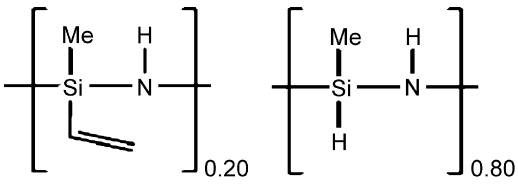


Fig. 1. The structure of the polysilazane precursor Ceraset® VL20 as provided in Ref. [16]

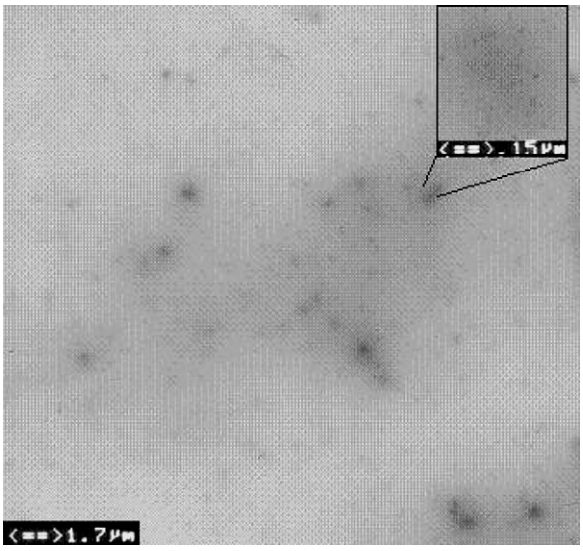


Fig. 2. TEM micrograph of silver nanoparticles embedded in a cross-linked polysilazane matrix. The inset shows that the dark regions consist of nanoparticle aggregates.

performed by a modified literature method as described in the experimental part.[6,7] Determination of the particle diameters using powder XRD and the Scherrer-formula gave an average particle size of about 10 nm. This is slightly larger than the values of 5–7 nm obtained from TEM images. Although the silver nanoparticles were protected and stabilized by oleylamine it turned out to be difficult to obtain a completely homogenous distribution in the precursor polymer. According to the TEM-observations (Fig. 2), the mixing procedure as described in the experimental section leads to small (∼100 nm) aggregates of silver nanocrystals surrounded by the cross-linked precursor polymer matrix.

The distance between individual particles within a nanoparticle aggregate is >10 nm, which is larger than the distances observed for oelylamine-stabilized silver nanoparticles without the polysilazane.[6] This indicates a further encapsulation and stabilization of the silver particles by polymer molecules or even a ligand exchange between the –NH– groups of the oleylamine with those of the polysilazane. Therefore, we decided to use this precursor system for cross-linking and pyrolysis experiments.

1,1′-Azo-1-bis(cyclohexanecarbonitrile) – a well known radical starter – was used to cure the precursor at 150 °C as described in the experimental part. The azo compound melts and decomposes at 110–116 °C forming alkyl radicals, which initiate cross-linking reactions. Alternatively, thermal cross-linking at 290 °C was applied. Pyrolysis of bulk and film samples was performed similar to the studies with the silver-free Ceraset®-derived samples,[17] followed by characterization of the *nc*-Ag/Si(C)N nanocomposites.

### 3.2. Characterization of the silver nanoparticles in the Si/C/N-matrix

The polymer-to-ceramic transition at elevated temperatures does not significantly influence the size of the silver nanoparticles as indicated by XRD (Fig. 3) and UV–vis measurements (Fig. 4). The XRD pattern taken for a bulk *nc*-Ag/Si(C)N sample shows a very broad (1 1 1) reflection of the *fcc* Ag nanocrystallites. The width of this reflection gave an average size of 5–7 nm, using Scherrer's equation which is in good agreement with TEM-observations (Fig. 5). The sample treated at 1200 °C reveals sharper (1 1 1) reflection due to grain growth.

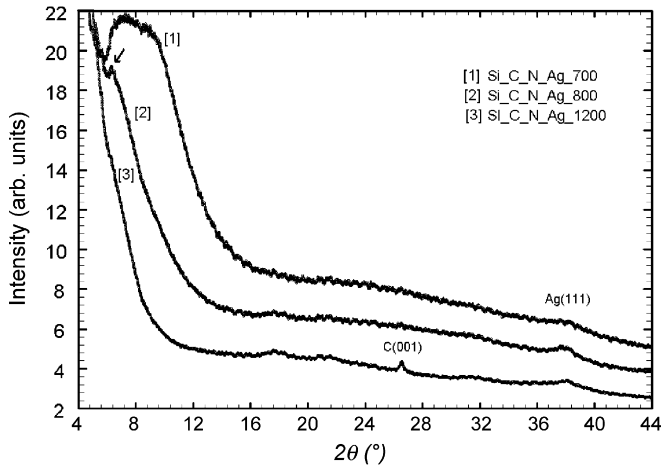


Fig. 3. X-ray diffraction patterns of silver containing polysilazane-derived nanocomposites after pyrolysis at various temperatures under flowing nitrogen ((1) 700 °C; (2) 800 °C; (3) 1200 °C).

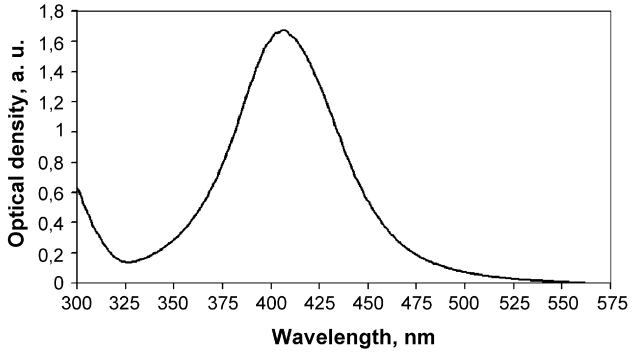


Fig. 4. Typical UV–vis spectrum of a yellow *nc*-Ag/SiCN composite exhibiting an SPR peak with a maximum at 405 nm caused by the silver nanoparticles.

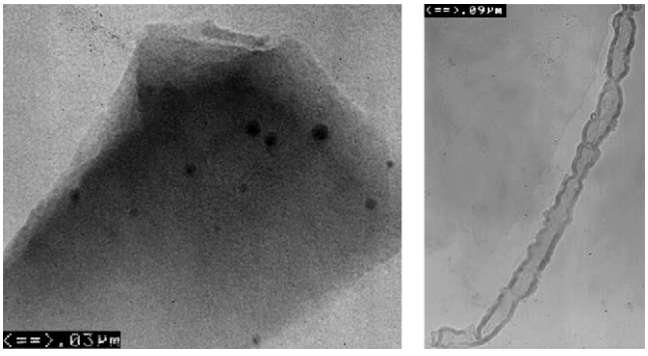


Fig. 5. TEM images of silver nanoparticles in the polymer-derived ceramic matrix (left). Carbon nanotube formed during the polymer-to-ceramic pyrolytic conversion (right).

UV–vis spectra of composite coatings on quartz glass substrates (Fig. 4) show a typical surface plasmon resonance (SPR) peak with a maximum at 405 nm, which also corresponds well to the particle size as derived from the XRD and TEM (Fig. 5) investigations. It causes a yellow color if the matrix is colorless or transparent.

Neither SPR peaks nor any XRD signals for crystalline silver were found for very thin (<1 μm) coatings that had been subjected to temperatures higher than 900 °C in flowing ammonia. This is most likely a consequence of the evaporation of silver ($mp_{bulk\ silver}$ = 962 °C), a similar phenomenon was also observed for sol–gel-derived silver-containing composites.[1]

The number density of silver particles in the Si/C/N matrix was calculated on the basis of a weight content of 3% Ag in the precursor polymer (see Section 2), a ceramic yield of 83% (vide infra), a bulk density of 2.2 g/cm$^3$ typically found for amorphous Si/C/N ceramics[15] and a density of 10.5 g/cm$^3$ for the silver. These data results in a volume content of 0.76% silver in the *nc*-Ag/SiCN composites. Assuming monodisperse spherical silver particles with 6 nm diameter a number density of $6.7 \times 10^{16}$ Ag particles/cm$^3$ is calculated. For other particle sizes of 8 or 4 nm number densities of $2.8 \times 10^{16}$ and $22.7 \times 10^{16}$ Ag particles/cm$^3$ are found, respectively.

### 3.3. Characterization of the Si/C/N matrix

For all pyrolysis temperatures, no significant differences between the FT-IR spectra (not shown here) of the *nc*-Ag/SiCN composites and SiCN reference samples without silver were found, indicating inertness of the silver nanoparticles to the matrix. Similarly, TGA studies showed almost complete polymer-to-ceramic transition at 800 °C with a yield of 83%, which is close to the value of 81.6% observed for fully cross-linked silver-free Ceraset®.[17] This result is crucial because of the silver evaporation and crystal growth at higher temperatures mentioned above.

The XRD measurements of samples obtained at 800 °C showed in addition to the above discussed (1 1 1) reflection for the silver nanoparticles a relatively sharp signal at a low 2$\theta$-value of 4.9–6.5°, corresponding to a *d*-spacing of 14–17 Å (Fig. 3). Products pyrolysed at 700 °C revealed stronger scattering in this region, i.e. a much broader signal at 6–11° 2$\theta$. At higher temperatures (1200 °C) the signal disappeared. These reproducible results may be attributed either to metastable intermediate cluster formation or to pores which close due to matrix shrinkage. The closure of pores at the same temperature region was reported for other polymer-derived SiCN-[15] and SiCO-materials.[19]

Besides, at 1200 °C graphitic carbon is formed as indicated by the black color of the products as well as the (0 0 0 1) reflection shown in Fig. 3. This carbon formation is common for many carbon-containing silazanes if pyrolysed under argon or nitrogen atmospheres. Pyrolysis under ammonia leads to colorless samples with lower carbon content or even carbon-free $SiN_x$-materials due to methane formation.[15] Very similar results were obtained with cross-linked silver nanoparticle—Ceraset® bulk samples and coatings.

Interestingly, nanotubes were also observed in some TEM images (Fig. 5). Carbon nanotube formation upon polymer pyrolysis was previously reported.[20] Nickel, cobalt and iron are usually catalytically active in nanotube synthesis. However, in our case it appears that the silver nanoparticles induce the nanotube formation, since metal-free samples did not contain any tubes. Nevertheless, clear evidence for this hypothesis – such as silver nanoparticles enclosed inside of a nanotube – was not found.

### 3.4. Biological tests

Antibacterial drop-tests of our *nc*-Ag/Si(C)N composite coatings pyrolysed at 800 °C clearly indicated strong antibacterial activity against Gram-positive (*S. aureus*) and Gram-negative (*E. coli*) bacteria (Fig. 6). It is known that very low concentrations of silver ions are responsible for this effect.[1] Thus, the elemental silver enclosed in the Si(C)N matrix is obviously oxidized to form silver cations which are very slowly released at the surface of the ceramic material:

$$Ag^0 \rightarrow Ag^+ + e^-$$

It remains an open question which species are acting as oxidizing agents. The presence of nitrogen as a relative electronegative element may accept the electrons forming $R_2N^-$-sites within the matrix. The latter effect may also help to support the diffusion of $Ag^+$ ions through the SiCN matrix providing higher mobility of silver.

However, oxidation of elemental silver might also occur directly on the surface. Due to the very small size of the nanoparticles there should be a large number of particles at the surface causing the antibacterial activity of the nanocomposite. For silver particles with diameters of <8 nm we calculated a particle number surface density of $>1.5 \times 10^{10}$ Ag particles/cm$^2$. The calculation is based on the assumption that monodisperse spherical silver particles are present. Those spheres which are in direct contact to the surface or sticking in the matrix at least for 2 nm were taken into account.

After a treatment of the composite ceramic surface with nitric acid, which should dissolve all silver particles in contact to the


Fig. 6. Agar plates after incubation with solutions of *S. aureus*. The reference sample (left) clearly shows colonies while the sample which was in contact with a *nc*-Ag/SiCN nanocomposite is free of any bacteria colonies (right).

solution, the antibacterial activity is still present. Thus, there must be a sufficient transport of silver from the Ag-particles protected/covered by the ceramic matrix to the surface. $[AgL_2]$-complex formation – possibly in part accompanied by hydrolysis of the matrix – can play a role for the mobilization of the silver. It is well known that silicon nitride as well as Si(C)N ceramics slowly react with water forming ammonia which forms a stable complex with the silver ions, thus dissolving hardly soluble silver salts such as AgCl:

$$Si_3N_4 + 6H_2O \rightarrow 3SiO_2 + 4NH_3$$

$$AgCl(s) + 2NH_3 \rightarrow [Ag(NH_3)_2]^+ + Cl^-$$

However, it is also well known that other silver-containing composite materials – e.g. organic polymer matrix systems based on polyurethane,[21] poly-vinyl-methyl-ketone[22] or chitosan[23] – which do not provide any *molecular* ligands for silver complex formation, also show antibacterial activity. Obviously, any matrix of a silver containing material seems to provide sufficient mobility of silver species to show biocide properties. The potential of this characteristic for applications of polymer-based silver-containing composites has been recognized, since products such as household appliances, textiles or medical devices are already available or under development.[24]

## 4. Conclusions

Silver–ceramic nanocomposites can be produced by combining well established synthesis procedures for noble metal nanoparticles and polymer-derived SiCN-ceramics. The advantages of preceramic-precursor techniques allows the preparation of bulk ceramics, coatings and other shapes using commercially available silazanes. The obtained materials consist of silver nanoparticles distributed in a silicon (carbide) nitride matrix. These materials reveal bactericide activity against Gram-negative (*E. coli*) and Gram-positive (*S. aureus*) bacteria. The simplicity and versatility of shaping techniques combined with the very high anti-bacterial activity of the *nc*-Ag/Si(C)N materials might lead to applications in biomedical, food as well as other industries.

## Acknowledgements

This work was supported financially in the framework of the Research Priority Programme of the State of Baden-Wuerttemberg (Project-title: Functional Materials; subproject: Polymer-Derived Metal-Ceramic Nanocomposites). The authors are grateful to Christine Dittrich for TEM-measurements and Margarete Kreuer-Ullmann for help with antibacterial tests.

## References

1. Korroris, M., Trapalis, C. C., Kossionides, S., Vlastou, R., Nsouli, B., Groetzschel, R. *et al.*, RBS and HIRBS studies of nanostructured $AgSiO_2$ sol–gel thin coatings. *Nucl. Instrum. Meth. Phys. Res. B*, 2002, **188**, 67–72.
2. Catauro, M., Raucci, M. G., De Gaetano, F. and Marotta, A., Antibacterial and bioactive silver-containing $Na_2O{\cdot}CaO{\cdot}2SiO_2$ glass prepared by sol–gel method. *J. Mater. Sci.: Mater. Med.*, 2004, **15**, 831–837.
3. Fu, G., Vary, P. S. and Lin, C.-T., Anatase $TiO_2$ nanocomposites for antimicrobial coatings. *J. Phys. Chem. B*, 2005, **109**, 8889–8898.
4. Kawashita, M., Tsuneyama, S., Miyaji, F., Kokubo, T., Kozuka, H. and Yamamoto, K., Antibacterial silver-containing silica glass prepared by sol–gel method. *Biomaterials*, 2000, **21**, 393–398.
5. Kato, T. and Takemura, Y., Antibacterial ferrite ceramic materials for suppressing bacterial propagation in water tanks. *Japanese Patent* 001831 A2, January 5, 2006, 6 pp.
6. Hiramatsu, H. and Osterloh, F. E., A simple large-scale synthesis of nearly monodisperse gold and silver nanoparticles with adjustable sizes and with exchangeable surfactants. *Chem. Mater.*, 2004, **16**, 2509–2511.
7. Wiley, B., Sun, Y., Mayers, B. and Xia, Y., Shape-controlled synthesis of metal nanostructures: the case of silver. *Chem. Eur. J.*, 2005, **11**, 454–463.
8. Pastoriza-Santos, I. and Liz-Marzan, L. M., Formation of PVP-protected metal nanoparticles in DMF. *Langmuir*, 2002, **18**, 2888–2894.
9. Chen, M., Liu, J. P. and Sun, S., One-step synthesis of FePt nanoparticles with tunable size. *J. Am. Chem. Soc.*, 2004, **126**, 8394–8395.
10. Reviews;
(a) Bradley, J. S. and Schmid, G., Noble metal nanoparticles. *Nanoparticles*, 2004, **186–199**, 230–238;
(b) Okura, I., Noble metal nanocolloids. *Encyclopedia Nanosci. Nanotechnol.*, 2004, **8**, 41–48;
(c) Tan, Y., Li, Y. and Zhu, D., Noble metal nanoparticles. *Encyclopedia Nanosci. Nanotechnol.*, 2004, **8**, 9–40;
(d) Schmid, G., ed., *Nanoparticles: From Theory to Application*. Wiley–VCH, Weinheim, 2004, p. 434.
11. Reviews;
(a) Andersen, P. C. and Rowlen, K. L., Brilliant optical properties of nanometric noble metal spheres, rods, and aperture arrays. *Appl. Spectrosc.*, 2002, **56**, 124A–135A;
(b) Kelly, K. L., Jensen, T. R., Lazarides, A. A. and Schatz, G. C., Modeling metal nanoparticles optical properties. *Met. Nanopart.*, 2002, 89–118.
12. Reviews;
(a) Narisawa, M., Polymer pyrolysis. *Mater. Eng.*, 2005, **28**, 491–508;
(b) Weinmann, M., Organosilicon polymers as precursors for ceramics. *Mater. Eng.*, 2005, **28**, 439–490;
(c) Greil, P., Polymer derived engineering ceramics. *Adv. Eng. Mater.*, 2000, **2**, 339–348;
(d) Ziegler, G. and Suttor, D., Engineering ceramics from preceramics polymers. *Key Eng. Mater.*, 1999, **161–163**, 103–106;
(e) Riedel, R., Advanced ceramics from inorganic polymers. *Mater. Sci. Technol.*, 1996, **17B**, 1–50.
13. Roewer, G., Herzog, U., Trommer, K., Mueller, E. and Fruehauf, S., Silicon carbide—a survey of synthetic approaches, properties and applications. *Struct. Bonding*, 2002, **101**, 59–135.
14. Zank, G. A., Preceramic polymer-derived silicon oxycarbides. *Silicon-containing Polymers*., 2000, pp. 697–726.
15. Kroke, E., Li, Y.-L., Konetschny, C., Lecomte, E., Fasel, C. and Riedel, R., Silazane-derived ceramics and related materials. *Mater. Sci. Eng. R*, 2000, **26**, 97–199.
16. A data sheet for the Si/C/N precursor polymer used in this study is available at: http://www.kioncorp.com/datasheets.html.
17. Li, Y.-L., Kroke, E., Riedel, R., Fasel, C., Gervais, C. and Babonneau, F., Thermal cross-linking and pyrolytic conversion of poly(ureamethylvinyl)silazanes to silicon-based ceramics. *Appl. Organomet. Chem.*, 2001, **15**, 820–832.
18. Chauhan, B. P. S., Rathore, J., Sardar, R., Tewari, P. and Latif, U., Synthesis, stabilization, and applications of nanoscopic siloxane–metal particle conjugates. *J. Organometall. Chem.*, 2003, **686**, 24–31.
19. Wilhelm, M., Soltmann, C., Koch, D. and Grathwohl, G., Ceramers–functional materials for adsorbtion techniques. *J. Eur. Ceram. Soc.*, 2005, **25**, 271–276.
20. (a) Berger, A., Pippel, E., Woltersdorf, J., Scheffler, M., Cromme, P. and Greil, P., Nanoprocesses in polymer-derived Si–O–C ceramics: electron

microscopic observations and reaction kinetics. *Phys. Status Solidi A: Appl. Mater. Sci.*, 2005, **202**, 2277–2286;
(b) Fan, Y., Wang, Y., Lou, J., Xu, S., Zhang, L., An, L. *et al.*, Formation of silicon-doped boron nitride bamboo structures via pyrolysis of a polymeric precursor. *J. Am. Ceram. Soc.*, 2006, **89**, 740–742.

21. Jain, P. and Pradeep, T., Potential of silver nanoparticle-coated polyurethane foam as an antibacterial water filter. *Biotechnol. Bioeng.*, 2005, **90**, 59–63.
22. Cioffi, N., Ditaranto, N., Torsi, L., Picca, R. A., De Giglio, E., Sabbatici, L. *et al.*, Analytical characterization and bioactivity of Ag and Cu nanoparticles embedded in poly-vinyl-methyl-ketone films. *Anal. Bioanal. Chem.*, 2005, **382**, 1912–1918.
23. Rhim, J. W., Hong, S. I., Park, H. M. and Ng, P. K., Preparation and characterization of chitosan-based nanocomposite films with antimicrobial activity. *J. Agric. Food Chem.*, 2006, **54**, 5814–5822.
24. (a) For medical devices, see e.g.: Furno, F., Morley, K. S., Wong, B., Sharp, B. L., Arnold, P. L., Howdle, S. M. *et al.*, Silver nanoparticles and polymeric medical devices: a new approach to prevention of infection? *J. Antimicrob. Chemother.*, 2004, **54**, 1019–1024;
(b) For several commercial applications of silver-containing coatings, see e.g.: Adams, L., Coatings: Safer Surfaces. In *Appliance Design*, 2006 (available under: http://www.appliancedesign.com/CDA/Articles/Feature_Article/).